ACS OMEGA

http://pubs.acs.org/journal/acsodf

Article

Functionally Graded Bioactive Composites Based on Poly(vinyl alcohol) Made through Thiol−Ene Click Reaction

Rajeswari K. Adarsh, Eva C. Das, Gopika V. Gopan, Shivaram Selvam, and Manoj Komath*

Cite This: *ACS Omega* 2022, 7, 29246−29255

Read Online

ACCESS | Metrics & More | Article Recommendations | Supporting Information

ABSTRACT: Functionally graded materials (FGMs) composed of a polymer matrix embedded with calcium phosphate particles are preferred for bone tissue engineering, as they can mimic the hierarchical and gradient structure of bones. In this study, we report the design and development of a FGM based on thiolated poly(vinyl alcohol) (TPVA) and nano-hydroxyapatite (nano-HA) with graded bioactivity, cell compatibility, and degradability properties that are conducive for bone regeneration. The polymer matrix comprises crosslinked poly(vinyl alcohol) with ester and thioether linkages formed via the thiol−ene click reaction, avoiding undesired additives and byproducts. Freshly precipitated and spray-dried HA was mixed with the TPVA hydrogel, and layers of varying concentrations were cast. Upon lyophilization, the hydrogel structure yielded porous sheets of the graded composite of TPVA and nano-HA. The new FGM showed higher values of tensile strength and degradation in phosphate buffer saline (PBS) *in vitro*, compared to bare TPVA. The bioactive nature of the FGM was confirmed through bioactivity studies in simulated body fluid (SBF), while cytocompatibility was demonstrated with human periodontal ligament cells *in vitro*. Cumulatively, our results indicate that based on the composition, mechanical properties, bioactivity, and cytocompatibility, the fabricated TPVA-HA composites can find potential use as guided bone regeneration (GBR) membranes.

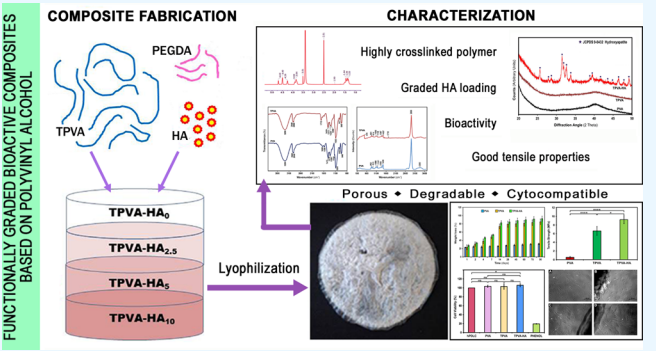

1. INTRODUCTION

Functionally graded materials (FGMs) are being extensively investigated for tissue engineering applications, as tissues in the body exist as a gradient structure to meet versatile functional requirements.[1] This is particularly true for hard tissue substitutes, as they have a hierarchical graded structure with anisotropic properties. In this regard, a scaffold designed with gradients in chemical composition, mechanical properties, and spatial distribution would be ideal for use in bone repair.[2] In the literature, several materials have been proposed for developing FGMs for tissue engineering applications. Some of these include polydimethylsiloxane and poly(ether) ether ketone composites, cellulose acetate−gelatin−boron-modified bioglass composition (as a bilayer membrane), electrospun chitosan and nano-HA (over amnion membranes), polycaprolactone and β-tricalcium phosphate (made as a scaffold through three-dimensional (3D) printing), and low-molecular weight chitosan with HA (as a three-layered membrane).[3−7] Among the various studies of FGM designs reported for biomedical applications, bioactive and biodegradable materials incorporating bioceramic composites are the most actively explored, as they can be effectively used to heal bony defects by enhancing the natural bone remodeling mechanism.

Of all the synthetic polymers explored for implantable FGMs, poly(vinyl alcohol) (PVA) appears to be very promising, as it possesses characteristics such as biocompatibility, nontoxicity, noncarcinogenicity, and ease of functionalization.[8] PVA, a linear polyol obtained through hydrolysis of polyvinyl acetate, is a long-chain polymer with a carbon backbone and pendent hydroxyl groups. Due to the presence of a large number of −OH groups, it is hydrophilic in nature with high solubility in aqueous solutions but insoluble in organic solvents.[9] The degree of hydrolysis or the percentage of −OH groups present in the polymer chain greatly influences its physicochemical and mechanical properties.[10] The physical characteristics and biocompatibility of PVA make it amenable for versatile applications, both as implants (e.g., hydrophilic coating over catheters, vascular embolic agents, nerve guides, cartilage replacement, tissue adhesion barriers, etc.) and nonimplantable devices (such as surgical sponges, eye-wetting drops, and contact lenses) alike.[10−12]

Received: May 31, 2022
Accepted: July 27, 2022
Published: August 15, 2022

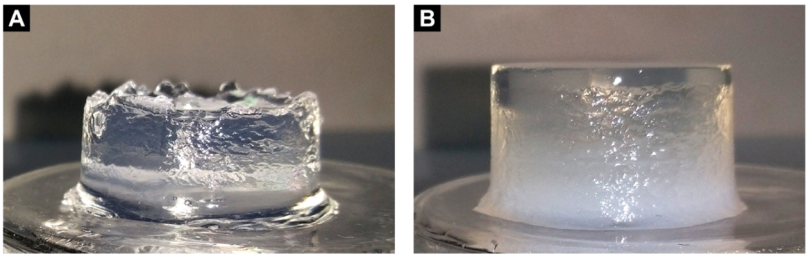

Figure 1. Images of the TPVA and TPVA-HA gels.

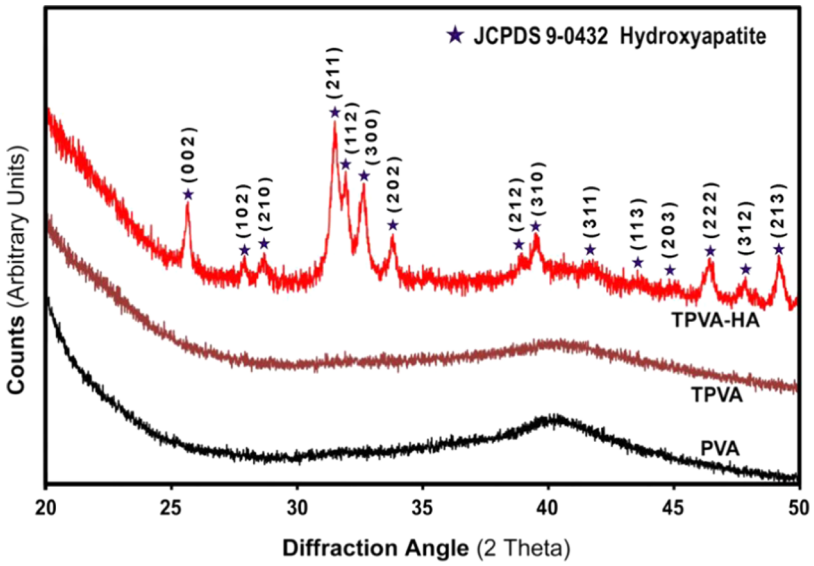

Figure 2. XRD spectra of poly(vinyl alcohol) (PVA), thiolated poly(vinyl alcohol) (TPVA), and thiolated PVA-HA composite (TPVA-HA).

For biomedical use, PVA is crosslinked through physical or chemical means to yield bulk hydrogels or membranes.[10,13,14] The physical crosslinking of PVA is done by the repeated freezing−thawing method, while chemical crosslinking is achieved by the formation of covalent bonds between the chains in an entangling manner.[15,16] Among the most widely used chemical crosslinking agents for PVA are monoaldehydes (acetaldehyde, formaldehyde) and dialdehydes (gluteraldehyde, glyoxal).[15] These aldehydes crosslink the PVA chains via acetal bridges between the pendent hydroxyl groups in the presence of sulfuric acid/acetic acid/methanol.[15] The major drawback with this type of crosslinking is that its time-consuming extraction procedures to remove the undesirable residues to maintain biocompatibility are very tedious. This problem can be solved by modifying PVA so that it can be crosslinked with high efficiency without free radical initiators. The click chemistry reaction is one such chemical-free approach to modify PVA.

Click chemistry-based reactions are characterized with high thermodynamic driving force, high yield, specificity (regio- and stereo-), and irreversibility.[17−19] Most notably, they generate minimal and benign byproducts, making these reactions green and biocompatible.[17−19] Some examples for click reactions include thiol−ene, [3 + 2] and [4 + 1] cycloaddition, Diels−Alder, thiol−yne, etc.[17−19] Among these, thiol−ene reactions or thiol−ene-mediated crosslinking is rather easy and straightforward. It can be carried out with a base-catalyzed mechanism or by the photon excitation method using photoinitiators along with thiol and ene.[20] The chemical reactions of PVA are quite similar to those of alcohols. For thiol−ene-mediated PVA crosslinking, PVA hydroxyl groups are alkene- or thiol-modified. Compared to alkene modification of PVA, thiol modification using thioglycolic acid (TGA) is preferred since it is a simple acid-mediated esterification reaction under aqueous conditions.[21] The thiol-modified PVA (TPVA) can be easily recovered and purified from the reaction mixture and can be easily crosslinked using water-soluble dialkene.[22]

The present work attempts to design implantable, bioactive, and functionally graded structures of PVA incorporated with hydroxyapatite (HA) via thiol−ene click chemistry for hard tissue repair applications. A thiol-bearing biocompatible polymer solution, when mixed with HA and a biocompatible diene crosslinker, forms a hydrogel intermediate, which can be dried into sheets with a composite structure that can be handled easily.

PVA was thiolated by acid-mediated esterification with a thiol-bearing carboxylic acid. The long-chain polymer with pendent thiol groups is crosslinked to form a gel using water-soluble dialkene. Esterification was selected to modify PVA, as it will help the composite material to degrade progressively and promote tissue regeneration *in vivo*. The bioactive HA is distributed in a graded pattern by a multiple-layer approach using a polymer−ceramic gel with varying concentrations of HA. The crosslinked gel FGM with graded concentrations of nano-HA was fabricated through layer-by-layer casting of the polymer crosslinker mix with varying amounts of nano-HA and converting to a porous composite membrane via freeze drying.

Extending click chemistry to generate a polymer−ceramic composite will ensure the biocompatibility of the material. The

https://doi.org/10.1021/acsomega.2c03382
ACS Omega 2022, 7, 29246−29255

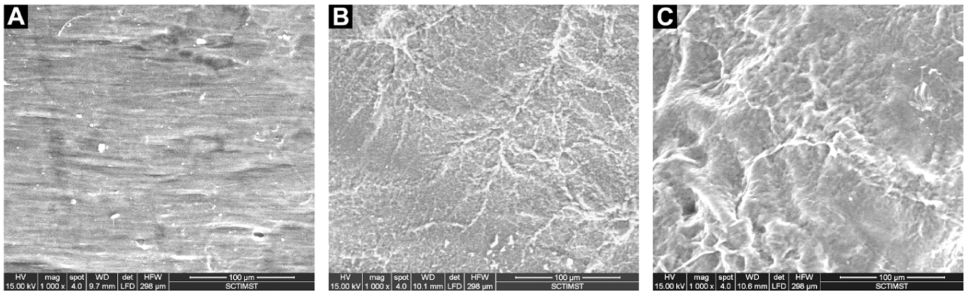

Figure 3. Scanning electron microscopy (SEM) images showing the surface features of (A) PVA, (B) TPVA, and (C) TPVA-HA composite.

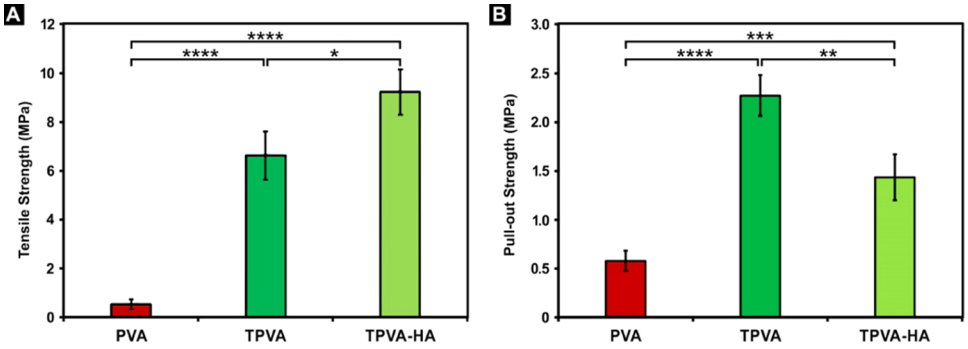

Figure 4. (A) Tensile strength of TPVA-HA composites. (B) Suture pullout strength of TPVA-HA composites.

FGM structure with graded bioactivity will be suitable for application at the interface of the bone and soft tissues, such as the treatment of periodontal defects in dentistry. With this specific application in mind, the material was tested for biocompatibility using human periodontal ligament cells *in vitro*.

2. RESULTS AND DISCUSSION

The synthetic polymer poly(vinyl alcohol) (PVA) was selected for the design and fabrication of functionally graded polymer−ceramic composite materials due to the ease of functionalization and its biocompatibility.[8] PVA was modified to a thiolated polymer so that it can be crosslinked with PEGDA along with a bioactive HA component via thiol−ene click chemistry. This provides a stereo−regio-specific crosslinking mechanism with a large thermodynamic drive, thereby leading to high yields. The functionalization of PVA to a partially thiol-modified derivative using TGA was confirmed from the spectroscopic techniques. Since the thiol modification reaction is a simple acid-catalyzed esterification reaction, it can be scaled up easily for viable industrial production.

2.1. Physical Appearance of the Graded Composite Gel. Figure 1A represents the gel without HA, and the composite gel obtained with graded HA addition is shown in Figure 1B. Figure 1B clearly shows the graded distribution of HA from top to bottom in the gel.

2.2. Characterization of TPVA-HA Functionally Graded Composites. *2.2.1. X-ray Diffraction Analysis of TPVA-HA Composites.* The presence of HA in the freeze-dried four-layered membrane was confirmed with XRD analysis of TPVA-HA, TPVA, and PVA samples. Figure 2 compares the XRD spectra of PVA, TPVA, and the TPVA-HA composite. The XRD patterns of PVA and TPVA showed a typical amorphous polymer. The XRD pattern of TPVA-HA showed slightly broadened peaks along with the amorphous peak of TPVA. The peaks obtained for TPVA-HA match with the ICDD (JCPDS-00-009-0432), which corresponds to nano-HA. This shows the existence of HA in the FGM without any phase change.

2.2.2. Micromorphology of TPVA-HA Composites. The morphology of the composite samples was visualized under a scanning electron microscope at 1000× magnification and is shown in Figure 3. Considering the surface morphology of the lyophilized sheets, PVA, TPVA, and TPVA-HA showed a nonporous surface, which is mainly due to a skin-like formation over the surface by the PVA polymer (Figure 3). The porous nature became evident after the thin skin over the surface degraded away, and the porous internal structure was clearly visible in samples subjected to a bioactivity test *in vitro* (Figure 7).

2.2.3. Mechanical Properties of TPVA-HA Composites. To qualify for biomedical applications, such as the periodontal barrier membrane, the FGM should have sufficient mechanical strength to withstand the forces acting on it while suturing. The results of the mechanical property evaluation (tensile strength and suture pullout strength) using a UTM are represented in Figure 4A,B. It is observed that crosslinking of PVA via the thiol−ene reaction increased the tensile strength from 0.538 ± 0.201 MPa, observed in PVA, to 6.645 ± 0.993 MPa, in crosslinked TPVA. The 12-fold increase in tensile strength is due to the crosslinked structure. In bare PVA, the noncovalent interaction of hydrogen bonds plays a major role in holding the polymeric chains. After thiolation and crosslinking, covalent crosslinking has also been formed between the polymer chains. This bonding interaction tightly keeps the polymer chains together, which is presumably the reason for the increase in tensile strength.[13] Incorporation of HA during the preparation of the composite further increased the strength of TPVA to 9.25 ± 0.925 MPa, that is, the presence of HA further increased the strength 1.4× compared to crosslinked TPVA (Figure 4A). The elastic modulus accessed from the tensile test was found to be 3.417 ± 0.232

https://doi.org/10.1021/acsomega.2c03382
ACS Omega 2022, 7, 29246−29255

MPa for PVA, 11.240 ± 0.944 MPa for TPVA, and 15.641 ± 0.504 MPa for TPVA-HA. Similar to the tensile strength, Young's modulus also got increased with the thiolation of PVA and addition of HA. The increase in Young's modulus on conversion of PVA to TPVA is due to the change of the noncovalent inter-polymeric chain interaction to a covalently bonded interaction. This can be correlated to the additional coordination interactions between the Ca^{2+} ions and OH^- in the HA particles and the residual −OH groups in the TPVA polymer via hydrogen bonds and ionic interactions.[23,24] All these attractive interactions collectively increase the strength of composite sheets. The results of tensile strength were comparable with those of the commercially available collagen-based membranes Bio-Gide (4.6 ± 0.94 MPa) and Ossix Plus (5.13 ± 2.48 MPa).[25]

However, the suture pullout strength was slightly contrary to the results observed for tensile strength. Figure 4B compares the mean suture pullout strength of the composite and control polymer. Similar to the trend observed for tensile strength, the suture pullout strength of crosslinked TPVA was observed to be higher than that of PVA. The increase in the suture pullout strength of TPVA compared to that of PVA is from the covalent crosslinking between the polymeric chains, and its magnitude is far greater than that of the noncovalent hydrogen bond interaction in pure PVA. However, with the addition of HA, about 37% decrease in strength was observed. The suture pullout strengths of TPVA and TPVA-HA were found to be 2.272 ± 0.212 and 1.435 ± 0.236 MPa, respectively. Since sutures have a small cross-section, pressure exerted at the interface of the thread and polymer will be very high, and this may be the reason for the suture pullout strength showing a less value compared to tensile strength. In the TPVA-HA composite, even though additional attractive interactions are present, pressure exerted at the interface of the thread and polymer may override them.

2.2.4. In Vitro Swelling of TPVA-HA Composites. 2.2.4.1. Water Uptake. *In vitro* swelling behavior of the materials in the sheet form is assessed and shown in Figure 5A. Compared to bare PVA, crosslinked TPVA and TPVA-HA showed more than 2.5-fold swelling. This high rate of swelling is mainly due to the increase in the hydrophilicity of PVA in its thiolated form.

2.2.4.2. Volume Swelling. *In vitro* swelling of the materials in the sheet form was assessed based on volume changes, and the results are shown in Figure 5B. For PVA sheets, the volume change was negligible, whereas the dimensional changes for TPVA and TPVA-HA samples were higher at any given time point.

The water uptake by TPVA and its composite with HA is more than that of bare PVA sheets. The dimensional swelling shows that PVA showed a significant increase in size, but for TPVA and TPVA-HA composites, the change in volume was nearly 300 times and with time decreased progressively. The increase in swelling is due to the increase in the hydrophilic nature of the polymer upon thiolation. The decrease in swelling after a definite time point must be due to the faster degradation of ester linkages in TPVA and TPVA-HA composites.

2.2.5. In Vitro Degradation of TPVA-HA Composites. The weight loss of samples on PBS aging is shown in Figure 6. Compared to PVA, the samples TPVA and TPVA-HA showed a high rate of degradation in terms of mass loss. The PVA sheets demonstrated 23% weight loss within 24 h, after which

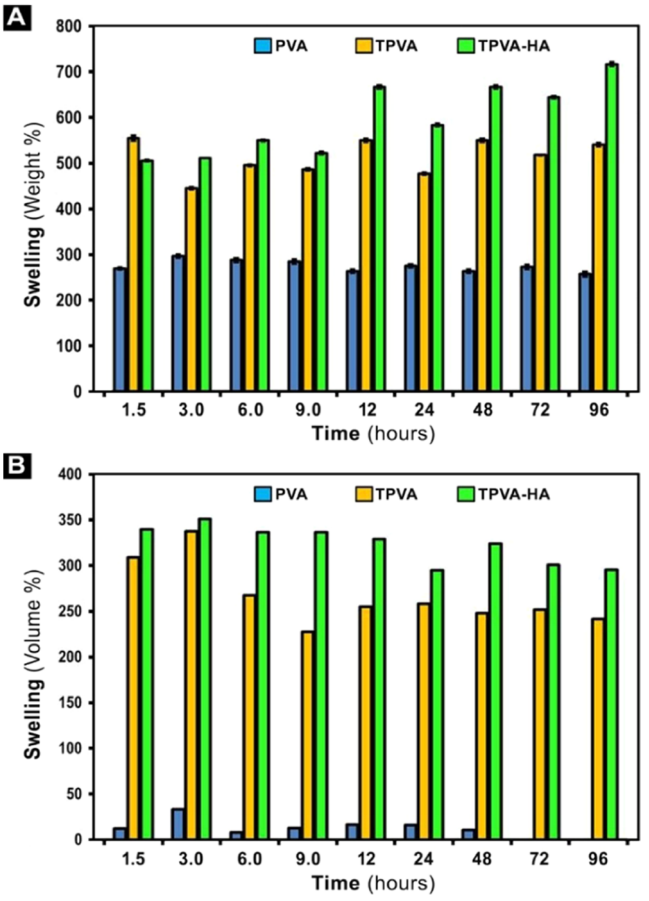

Figure 5. *In vitro* swelling study results on TPVA-HA composites. (A) Water uptake behavior and (B) dimensional changes.

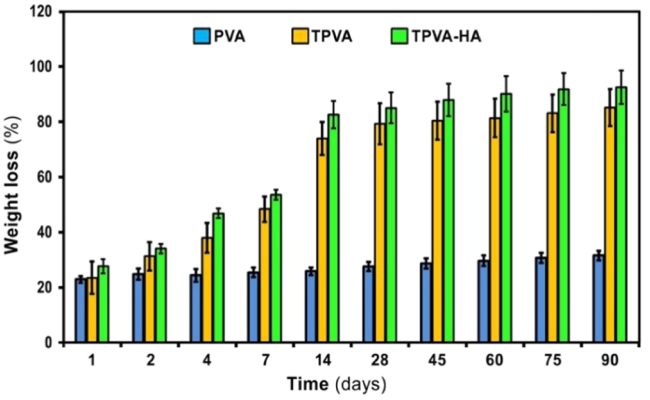

Figure 6. *In vitro* degradation study showing the percentage weight loss of TPVA-HA composites on PBS aging.

no significant mass loss was observed. However, in the case of crosslinked TPVA and the TPVA-HA composite, more than 50% weight loss was observed within one week. The weight loss was more prominent after 14 days with percentage values of 25, 74, and 82% for PVA, TPVA, and TPVA-HA composites, respectively (Figure 6). However, at 28 days, >85% weight loss was observed. The high rate of degradation in TPVA and TPVA-HA could be attributed to the hydrolysis of ester linkages in the polymer. The degradation of TPVA and TPVA-HA composites is quite similar, and the mass loss in PEGDA-crosslinked TPVA occurs via ester degradation. There are ester bonds between PVA and TGA in the TPVA backbone

https://doi.org/10.1021/acsomega.2c03382
ACS Omega 2022, 7, 29246−29255

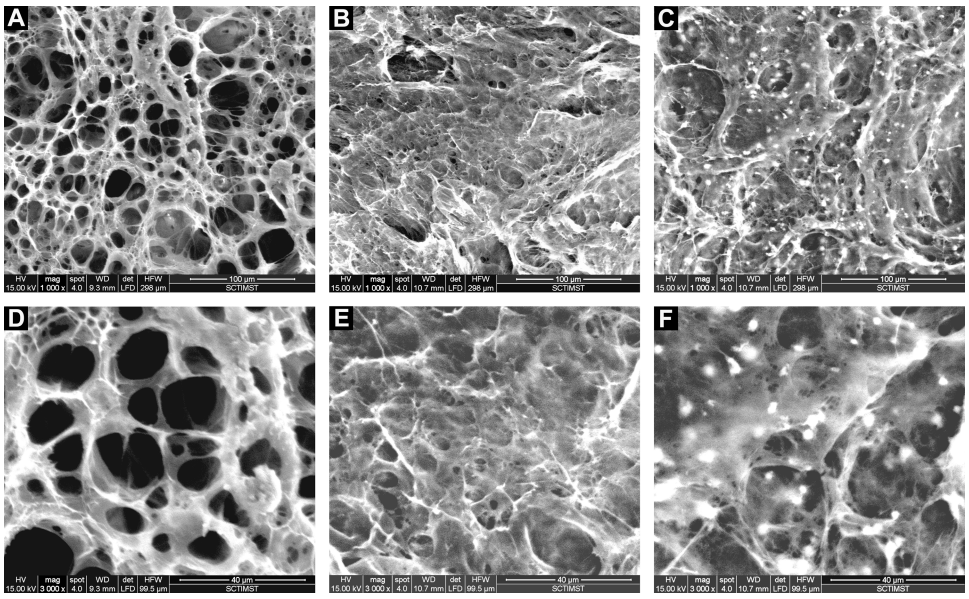

Figure 7. SEM images of TPVA-HA composites after immersing in SBF for 7 days along with PVA and TPVA as control materials. (A−C) PVA, TPVA, and TPVA-HA at 1000× magnification. (D−F) PVA, TPVA, and TPVA-HA at 3000× magnification.

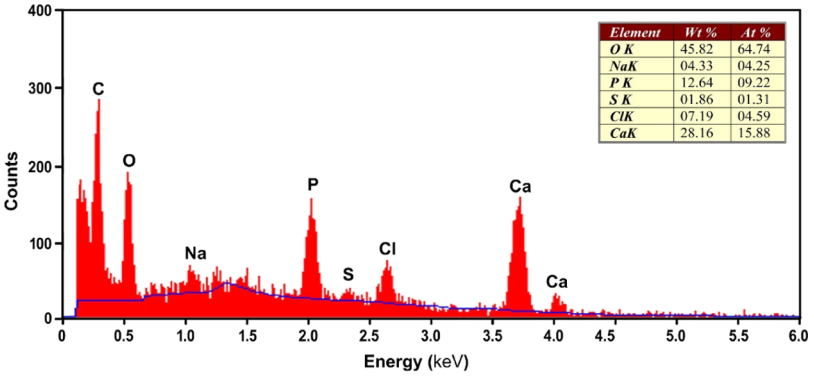

Figure 8. EDAX analysis of the sample surface of TPVA-HA after the bioactivity test (the SEM image of the sample could be found in Figure 7F).

and between acrylate and PEG in PEGDA. As far as covalent bonds are considered, ester bonds are more labile at physiological pH. This might be the reason why both TPVA and TPVA-HA underwent >70% degradation within 2 weeks. Of note, the degraded products are expected to be PVA, PEG, and 2,2′-thio-bis(acetic acid). Afterward, up to a period of 3 months, the degradation was complete with all the ester bonds getting cleaved away, leaving behind ∼10% of PVA, which is not prone to degradation through hydrolysis.

2.2.6. In Vitro Bioactivity Studies. The surface morphology of the sheets after immersing in SBF for 7 days is shown in Figure 7. For PVA, only surface degradation was observed. However, in the case of TPVA-HA sheets, apatite-like deposition was observed on the surface and inside the sheets. Energy-dispersive X-ray spectroscopic (EDAX) analysis of the deposited particles was carried out, and the results are shown in Figure 8. The Ca/P ratio obtained from the energy-dispersive system (EDS) analysis was approximately 1.72 (Figure 8).

In the *in vitro* bioactivity studies, PVA and TPVA samples without the HA content showed no apatite deposition over the surfaces. This result is not surprising, as there are no specific functional groups in these polymers to induce apatite formation. TPVA-HA composites revealed spherical globules of apatite crystals over and into the surface of the material after 7 days of immersion in SBF. The apatite-like deposition in TPVA-HA is only observed on the side of the graded composite having a high concentration of HA (Figure 7). Further confirmation of the deposited layer is obtained from EDS analysis of the particles (Figure 8). The EDAX data show a Ca/P ratio of 1.72 for the apatite-like deposition, which is within the range of apatitic ratios.[26,27] There was no apatite deposition on the other side of the graded composite, where HA was not present. It is evident from the results that the graded composite prepared *via* layer-by-layer gel casting gives a gradation in bioactivity to the composite. The Na^+ and Cl^- peaks observed in the EDS spectra come from the SBF solution in which the bioactivity test was performed.

2.2.7. In Vitro Cytocompatibility. 2.2.7.1. MTT Assay. Figure 9 represents the results of MTT assay using hPDL cells showing the percentage cell viability of PVA, TPVA, and TPVA-HA materials. All the samples showed ∼100% cytocompatibility.

2.2.7.2. Direct Contact. The cytocompatibility of the materials with hPDL cells was evaluated using the direct contact test. The results of direct contact assay are shown in Figure 10. The hPDL cells cultured in direct contact with the test materials showed no evidence of cytotoxicity such as

https://doi.org/10.1021/acsomega.2c03382
ACS Omega 2022, 7, 29246−29255

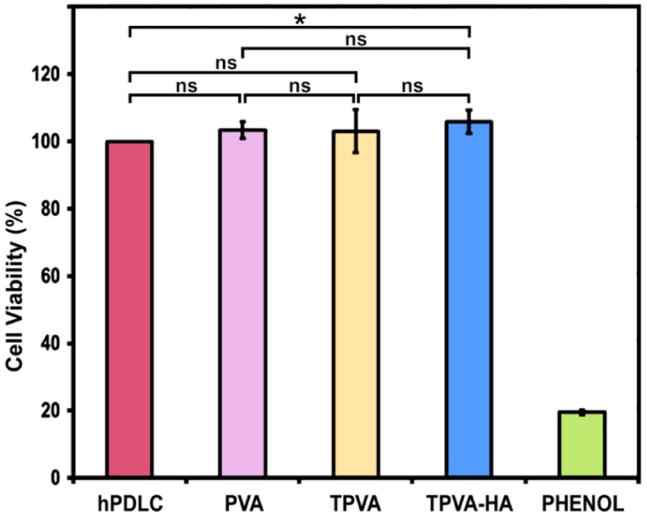

Figure 9. MTT assay of materials using hPDL cells.

detachment from the surface or loss of morphology. The cells were seen to be adherent and maintained their spindle morphology, both in the cell control and in the presence of PVA, TPVA, and TPVA-HA sheets.

2.2.7.3. Cell Adhesion and Proliferation Actin Staining. The confocal laser scanning microscopy (CLSM) images of the actin cytoskeleton-stained hPDL cells are shown in Figure 11. The CLSM images of the hPDL cells on the membranes showed typical spindle morphology as compared to the control cells cultured on cover glass. In addition, the periodontal ligament fibroblasts cultured on the membranes showed a three-dimensional distribution, showing migration of cells into the membranes.

The *in vitro* cytotoxicity of materials evaluated *via* MTT assay and the direct contact test using hPDL cells proves that the materials are noncytotoxic in nature. In the direct contact test, no morphological changes were observed in cells that were in contact with the composite material (TPVA-HA) and the control materials (TPVA and PVA) (Figure 10). The quantification of cell viability based on MTT assay showed that almost all cells that were in contact with the sheets of PVA, TPVA, and TPVA-HA were viable (Figure 9). The cell adhesion and spreading studies using confocal microscopy further substantiate the results of MTT and direct contact assay (Figure 11).

3. CONCLUSIONS

The present work introduces an effective and viable method of production of functionally graded bioactive composites based on poly(vinyl alcohol) for tissue engineering applications *via* the thiol−ene click reaction. Thiolated PVA was prepared to make it a click chemistry-based crosslinkable polymer, and to that end, successful conjugation of thiol groups *via* esterification was performed and confirmed *via* Fourier transform infrared (FTIR), FT-Raman, and ^{1}H NMR analyses. The crosslinking mechanism used was a base-catalyzed Michael addition of thiol with -ene to form a thioether linkage, which avoids undesired byproducts and free radical initiators in the hydrogel fabrication process. The reaction has a large thermodynamic drive, ensuring full crosslinking. The thiol−ene crosslinking when mixed with PEGDA was also confirmed through spectroscopy. The thiol−ene crosslinking of the polymer−ceramic−crosslinker mixture followed by freezing and subsequent lyophilization resulted in a composite in which the bioactive HA component is distributed in a graded manner across the thickness.

The FGM obtained in the sheet form was found porous in the SEM analysis, and it showed higher tensile strength than that of the bare material. The *in vitro* bioactivity test in simulated body fluid showed apatitic layer formation on the side where the HA particles are present. The material showed degradation properties in PBS, with a weight shedding of more than 80% within 14 days. The degradation data ensure the material to resorb *in vivo* under physiological conditions after its intended function. The FGM was found noncytotoxic in the direct contact test using human periodontal ligament cells. The

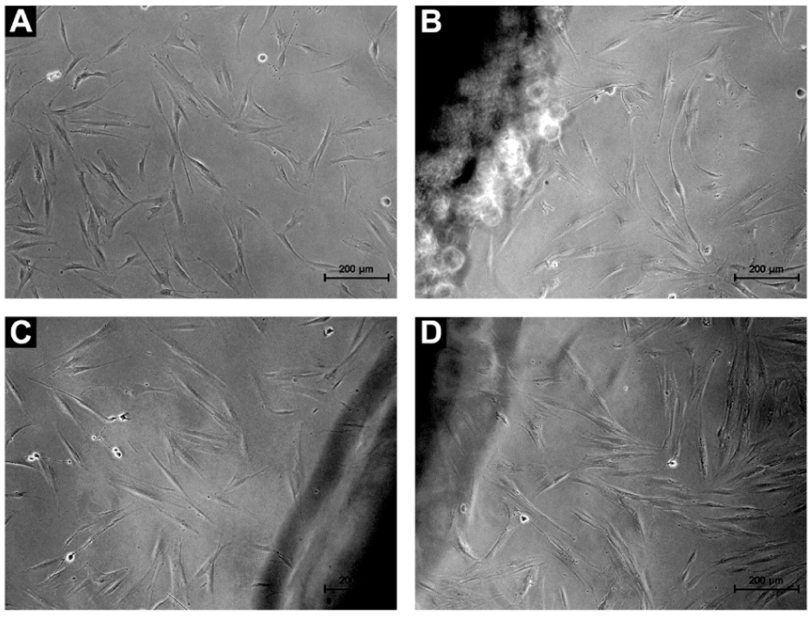

Figure 10. Direct contact assay of materials using hPDL cells for 24 h. (A) Cells alone, (B) PVA sheet, (C) TPVA sheet, and (D) TPVA-HA sheet.

https://doi.org/10.1021/acsomega.2c03382
ACS Omega 2022, 7, 29246−29255

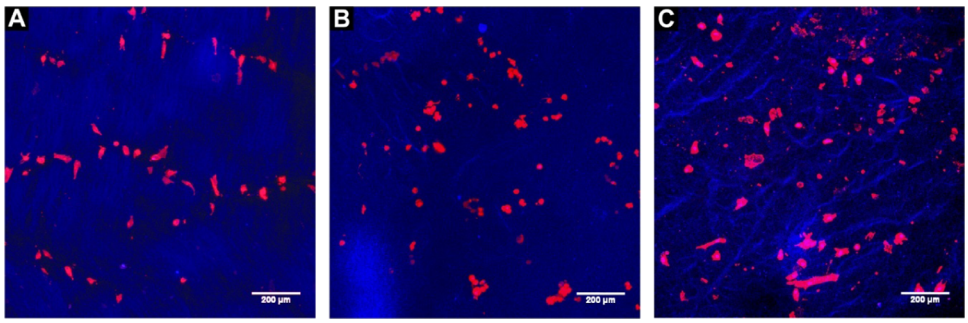

Figure 11. Confocal laser scanning microscopy images showing actin staining on sheets cultured with hPDL cells for 24 h, (A) PVA, (B) TPVA, and (C) TPVA-HA (scale bar: 200 μm).

cytocompatibility was established through cell viability tests. This kind of functionally graded, bioactive, degradable, cytocompatible material in the sheet/membrane form will be an ideal choice for guided tissue regeneration applications, specifically in the management of periodontal defects.

4. EXPERIMENTAL SECTION

4.1. Materials and Methods. To develop the polymer−ceramic composite with a graded concentration of HA, a gel-based approach was adopted. A four-layered composite of TPVA with each layer having a specific wt % of HA in the diminishing order (10, 5, 2.5, and 0%) was made via layer-by-layer gel casting. The TPVA-HA composite gel was prepared by mixing a dispersion of TPVA and HA with PEGDA crosslinker at neutral pH. The reaction proceeds by the base-catalyzed Michael addition route. At neutral pH, ionization of thiol groups will be higher and hence is readily attacked by the alkene groups of PEGDA. The crosslinking between TPVA and PEGDA was confirmed from FTIR analysis (Figure S5A). The reaction scheme for TPVA synthesis along with the mechanism of thiol−ene crosslinking that results in gel formation is shown in Figure S6

4.1.1. Fabrication of the TPVA-HA Functionally Graded Composite. The TPVA-HA composite with a graded composition of HA was prepared via layer-by-layer casting of polymer−ceramic−crosslinker pregel suspension in Petri plates. The composition of the HA was adjusted at a concentration of 0−10% (m/m) to the dry weight of TPVA polymer. Three different TPVA-HA suspensions were made by dispersing 13, 26, and 56 mg of HA to 10 mL of 5% (m/v) aqueous TPVA solution in three separate beakers. To about 5 mL of each TPVA-HA suspension, 1.25 mL of 6.25% (v/v) aqueous solution of PEGDA was added and mixed homogeneously. Each pregel mixture is poured one over another in the descending order of HA concentration. The four-layered gel thus prepared has the first layer with HA 10% m/m to the polymer (TPVA-HA_{10}), the second layer with HA 5% m/m to the polymer (TPVA-HA_5), the third layer with HA 2.5% m/m to the polymer (TPVA-$HA_{2.5}$), and the final fourth layer (top layer) with HA 0% m/m to the polymer (TPVA-HA_0). After complete gelation, the plates containing gel were cooled to −20 °C and freeze-dried. The porous membrane thus obtained is designated as TPVA-HA. The control material is also prepared in the same manner by avoiding HA and is designated as TPVA-HA_0.

4.1.2. Characterization of the TPVA-HA Functionally Graded Composite. 4.1.2.1. X-ray Diffraction Analysis. The presence of HA in the FGM was confirmed from XRD analysis using a Bruker D8 Advance X-Ray diffractometer with Cu Kα radiation generated at a voltage of 40 kV and a current of 30 mA. The spectra were recorded in the 2θ range of 10−50° at a rate of 4 °/min. The diffraction data were then compared with the standard ICDD data to identify the phase of calcium phosphate.

4.1.2.2. Scanning Electron Microscopy. The morphological changes on converting PVA to TPVA and then to the crosslinked polymer−ceramic composites were investigated using scanning electron microscopy (SEM, Hitachi, S-2400). The samples were dried and sputter-coated with gold before loading in SEM.

4.1.2.3. Mechanical Testing. To evaluate the effect of crosslinking in altering the mechanical properties of the polymer, the tensile test and suture pullout test were conducted. The tensile test was performed using a universal testing machine (UTM model, Instron 3345, U.K.) as per the standard ISO 527-3. Samples of 0.5 mm average thickness were cut into a size of 5 cm × 1 cm (n = 12), fitted using appropriate fixtures, and subjected to tensile force vertically at the speed of 20 mm/min. Measurements were done using a load cell of 100 N up to the point of sample failure. The tensile strength and elongation of samples were determined from the data.[28]

The suture pullout strength represents the tear-off limit when a suture thread passing across the membrane is pulled out. Samples of 10 mm width and 45 mm length (n = 12) were cut out, and the bottom end was gripped onto the lower jaw of the UTM. A single suture was tied on the top end with monofilament silk suture thread, at 5 mm down from the top edge along the middle line. The suture ends were folded and gripped to the upper jaw of the UTM fixture and pulled at a rate of 10 mm/min. The tearing of the membrane was taken as the end point.[28]

4.1.2.4. In Vitro Swelling, Water Uptake, and Dimensional Change. *In vitro* swelling based on water uptake and dimensional changes of TPVA-HA was analyzed in PBS saline (pH 7.4) at a temperature of 37 ± 0.5°C. Preweighed membranes of 2 cm × 2 cm (n = 6) dimension were kept immersed in 5 mL of 1 × PBS and taken out at different time points (0, 0.25, 0.5, 1, 24, and 48 h). Surface water was wiped out using tissue paper, and weight gain and dimensional changes were measured. The percentage swelling in terms of water uptake was calculated using the formulae.[28,29]

$$\text{swelling by weight\%} = \{(W_f - W_i) \times 100\}/W_i$$

$$\text{swelling by volume\%} = \{(V_f - V_i) \times 100\}/V_i$$

https://doi.org/10.1021/acsomega.2c03382
ACS Omega 2022, 7, 29246−29255

where W_i, W_f, V_i, and V_f are the initial weight, final weight, initial volume, and final volume of the composite, respectively.

4.1.2.5. In Vitro Degradation. *In vitro* degradation of the preweighed TPVA-HA composite sheets ($n = 6$) of 1 cm × 1 cm dimension was tested over a period of 3 months by immersing in phosphate-buffered saline (PBS) having a pH of 7.4 maintained at 37 ± 0.5°C temperature. After each time point, the membrane was collected from the PBS medium, washed thoroughly with distilled water, and dried in vacuum till a constant weight is obtained and then placed back to the respective wells, and the process was continued. The percentage weight loss at each time point was estimated using the formula.[28]

$$\%\text{weight loss} = \{(W_i - W_f) \times 100\}/W_i$$

where W_i and W_f are the dry weights of the membrane at the initial and final time periods, respectively.

4.1.2.6. In Vitro Bioactivity. The bioactivity test for the TPVA-HA composite membrane was carried out by immersing the preweighed membrane (1.5 cm × 1.5 cm) $n = 6$ in 10 mL of simulated body fluid (SBF) and maintained at 37 ± 0.5 °C for 3 and 7 days with SBF medium replacement every 2 days. The samples removed at definite time periods were thoroughly washed with deionized water and dried over silica gel until a constant weight was obtained. The bioactivity was then confirmed by analyzing the change in surface morphology using scanning electron microscopy and elemental composition of the deposited layer by energy-dispersive spectroscopy using an EDAX Genesis XM 4 integrated with the ESEM.[26]

4.1.2.7. In Vitro Cytocompatibility Studies. The cytocompatibility of the samples was evaluated through the direct contact method and MTT assay using human periodontal ligament (hPDL) cells. The cells were isolated from hPDL tissues collected from anonymous discarded extracted teeth following institutional ethical procedures. The cells were cultured in α-MEM, 10% FBS containing the antibiotics penicillin, streptomycin (100 IU), and amphotericin B (0.25 mg/100 mL) in a humidified incubator at 5% CO_2 at 37 ± 0.2 °C. The cells were characterized prior to the direct contact test and MTT assay. The confluent monolayer was subcultured and maintained for further studies. The samples (4 mm disc shape cut from 0.5 mm-thick membranes) were sterilized by autoclaving before the analysis.[28]

4.1.2.8. Direct Contact Test Using hPDL Cells. For direct contact cytotoxicity evaluation, hPDL cells were cultured in 24-well cell culture plates at 3×10^4 cells/well and cultured for 24 h. Then, the medium was discarded, and the samples (sterile discs of 4 mm diameter) were carefully placed over the cells and cultured for 24 h in α-MEM. The wells without the test materials were taken as the cell control (negative control), and those treated with 0.13% phenol were taken as the positive control. After 24 h, the wells were viewed under an inverted phase contrast microscope (Nikon), and the cell response was graded, based on the morphology, cell lysis, cell detachment, and vacuolization of the cells around the material. The grades were marked as 0 (no cytotoxicity), 1 (slight cytotoxicity), 2 (mild cytotoxicity), 3 (moderate cytotoxicity), and 4 (severe cytotoxicity).

4.1.2.9. MTT Assay Using hPDL Cells. The hPDL cells were seeded onto a 24-well cell culture plate (Nunc, Thermofischer) at a density of 3×10^4 cells/well and cultured for 24 h. Thereafter, the medium was discarded, and the sterile samples were carefully placed over the cell monolayer. The well with cells alone was taken as the cell control (negative control), and the well with 0.13% phenol served as the positive control (toxic control). After 24 h, the medium was discarded, and the cells were incubated in 200 μL of freshly prepared MTT solution (1 mg/mL) in the dark for 2 h. MTT assay was carried out to measure the mitochondrial cellular metabolism and is based on the capability of metabolically active hPDL cells to reduce the yellow water-soluble tetrazolium salt (MTT) to purple formazan crystals using the mitochondrial enzyme succinate dehydrogenase. The intensity of the purple color formed is proportional to the number of metabolically active cells. After 2 h, the MTT solution was discarded, and the formazan crystals formed were dissolved in isopropanol to measure the optical density (OD) spectrophotometrically at 570 nm. The percentage metabolic activity was calculated as per the formula

$$\text{percentage metabolic activity} = (\text{OD test}/\text{OD cell control}) \times 100$$

The values were plotted as mean ± standard deviation.

4.1.2.10. hPDL Cell Adhesion and Proliferation (Actin Cytoskeleton Staining). The functional evaluation of the composites was carried out using human periodontal ligament cells. Primary periodontal ligament cells (hPDL cells) at passage 3 were trypsinized using 0.25% trypsin and seeded onto the membranes at a cell density of 10^4 cells/cm^2. The cells were cultured in αMEM with 10% FBS. At 24 and 48 h, cells were fixed using 4% paraformaldehyde (PFA) for 1 h, washed with PBS, permeabilized with 0.1% triton X-100, and incubated with the Phalloidin-iFluor 555 reagent (Abcam) for 1 h in the dark. After 1 h, the unbound dye was washed off using PBS, and the cell nuclei were counterstained using Hoechst 33258 (0.05 μg/mL). The cytoskeleton-stained cells were viewed and imaged in a confocal laser scanning microscope (Nikon) at the excitation of 305 nm (Hoechst 33258) and 555 nm (Phalloidin-iFluor 555).

4.1.2.11. Statistical Analysis. The statistical significance of mechanical and cytocompatibility data was assessed by one-way analysis of variance (ANOVA) and *t*-test using GraphPad Prism 6.01; a p value of ≤ 0.05 is considered to be significant. The p values of < 0.05 and <0.01 are denoted by notations (*) and (**), respectively, and no significant difference (p value > 0.05) is denoted by ns. The data obtained were represented as means ± standard error (SE) with $n \geq 3$ samples/group for *in vitro* cytocompatibility studies, $n \geq 6$ for other *in vitro* studies (degradation, water uptake, swelling), and $n \geq 8$ samples/group for mechanical analysis.

■ ASSOCIATED CONTENT

Supporting Information

The Supporting Information is available free of charge at https://pubs.acs.org/doi/10.1021/acsomega.2c03382.

Synthesis and structural analysis of TPVA; synthesis and characterization of HA; preparation and characterization of the TPVA gel; FTIR and Raman spectra of PVA and TPVA; ^{1}H NMR analyses of PVA and TPVA; evidence for thiol substitution on TPVA; FTIR and XRD spectra of HA; characterization of thiol−ene-crosslinked TPVA gel; and reaction scheme of TPVA preparation and the mechanism of crosslinking (PDF)

https://doi.org/10.1021/acsomega.2c03382
ACS Omega 2022, 7, 29246−29255

AUTHOR INFORMATION

Corresponding Author

Manoj Komath − *Biomedical Technology Wing, Sree Chitra Tirunal Institute for Medical Sciences and Technology, Trivandrum 695012, India;* orcid.org/0000-0001-8576-5915; Email: manoj@sctimst.ac.in

Authors

Rajeswari K. Adarsh − *Biomedical Technology Wing, Sree Chitra Tirunal Institute for Medical Sciences and Technology, Trivandrum 695012, India*

Eva C. Das − *Biomedical Technology Wing, Sree Chitra Tirunal Institute for Medical Sciences and Technology, Trivandrum 695012, India*

Gopika V. Gopan − *Biomedical Technology Wing, Sree Chitra Tirunal Institute for Medical Sciences and Technology, Trivandrum 695012, India*

Shivaram Selvam − *Biomedical Technology Wing, Sree Chitra Tirunal Institute for Medical Sciences and Technology, Trivandrum 695012, India*

Complete contact information is available at: https://pubs.acs.org/10.1021/acsomega.2c03382

Author Contributions

Conceptualization, design and supervision of study, and critical revision for important intellectual content were contributed by M.K. Data curation, analysis, and interpretation of data and drafting the article were done by R.K.A., E.C.D., G.V.G., and S.S.

Notes

The authors declare no competing financial interest.

ACKNOWLEDGMENTS

The authors would like to thank the Director and the Head, Biomedical Technology Wing of SCTIMST for providing facilities for this work. The first author (R.K.A.) acknowledges the fellowship provided by the Department of Biotechnology, Government of India, from the project no. BT/PR14704. The second author (E.C.D.) acknowledges the research associate fellowship from the ICMR. The authors also express thanks to Dr. H.K. Varma, Dr. Roy Joseph, Dr. S. Suresh Babu, Dr. K.V. Nishad, Dr. Nimmy Mohan, and Dr. K.R. Remya for the technical support.

ABBREVIATIONS

FGM, functionally graded materials; TPVA, thiolated poly-(vinyl alcohol); HA, hydroxyapatite; PBS, phosphate buffer saline; SBF, simulated body fluid; GBR, guided bone regeneration; PVA, poly(vinyl alcohol); TGA, thioglycolic acid; HCl, hydrochloric acid; FTIR, Fourier transform infrared spectroscopy; GPC, gel permeation chromatography; EDAX, energy-dispersive X-ray spectroscopy; D_2O, deuterated water; DTNB, 5.5′-dithiobis (2-nitrobenzoic acid)]; $Ca(NO_3)_4 \cdot 4H_2O$, calcium nitrate tetrahydrate; $NH_4H_2PO_4$, ammonium dihydrogen orthophosphate; KBr, potassium bromide; XRD, X-ray powder diffraction; PEGDA, poly(ethylene glycol) diacrylate; SEM, scanning electron microscope; UTM, universal testing machine; hPDL, human periodontal ligament; αMEM, minimum essential medium α modification; MTT, 3-(4,5-dimethylthiazol-2-yl)-2,5-diphenyltetrazoliumbromide; CLSM, confocal scanning laser microscopy

REFERENCES

(1) Lowen, J. M.; Leach, J. K. Functionally graded biomaterials for use as model systems and replacement tissues. *Adv. Funct. Mater.* **2020**, *30*, No. 1909089.

(2) Li, S.; Demirci, E.; Silberschmidt, V. V. Variability and anisotropy of mechanical behavior of cortical bone in tension and compression. *J. Mech. Behav. Biomed. Mater.* **2013**, *21*, 109−120.

(3) Smith, J. A.; Mele, E.; Rimington, R. P.; Capel, A. J.; Lewis, M. P.; Silberschmidt, V. V.; Li, S. Polydimethylsiloxane and poly (ether) ether ketone functionally graded composites for biomedical applications. *J. Mech. Behav. Biomed. Mater.* **2019**, *93*, 130−142.

(4) Moonesi Rad, R.; Atila, D.; Evis, Z.; Keskin, D.; Tezcaner, A. Development of a novel functionally graded membrane containing boron-modified bioactive glass nanoparticles for guided bone regeneration. *J. Tissue Eng. Regener. Med.* **2019**, *13*, 1331−1345.

(5) Dhawan, S.; Takiar, M.; Manocha, A.; Dhawan, R.; Malhotra, R.; Gupta, J. Functionally graded membrane: A novel approach in the treatment of gingival recession defects. *J. Indian Soc. Periodontol.* **2021**, *25*, 411−417.

(6) Maruyama, M.; Pan, C. C.; Moeinzadeh, S.; Storaci, H. W.; Guzman, R. A.; Lui, E.; Ueno, M.; Utsunomiya, T.; Zhang, N.; Rhee, C.; Yao, Z.; et al. Effect of porosity of a functionally-graded scaffold for the treatment of corticosteroid-associated osteonecrosis of the femoral head in rabbits. *J. Orthop. Transl.* **2021**, *28*, 90−99.

(7) Qasim, S. S. B.; Baig, M. R.; Matinlinna, J. P.; Daood, U.; Al-Asfour, A. Highly Segregated Biocomposite Membrane as a Functionally Graded Template for Periodontal Tissue Regeneration. *Membranes* **2021**, *11*, 667.

(8) Kenawy, E. R.; Kamoun, E. A.; Eldin, M.; El-Meligy, M. A. Physically crosslinked poly(vinyl alcohol)-hydroxyethyl starch blend hydrogel membranes: Synthesis and characterization for biomedical applications. *Arabian J. Chem.* **2014**, *7*, 372−380.

(9) Barui, A. *Woodhead Publishing Series in Biomaterials*; Pal, K.; Banerjee, I., Eds.; Woodhead Publishing: Sawston, United Kingdom, 2018; Chapter 3, DOI: 10.1016/B978-0-08-102179-8.00003-X.

(10) Baker, M. I.; Walsh, S. P.; Schwartz, Z.; Boyan, B. D. A review of polyvinyl alcohol and its uses in cartilage and orthopedic applications. *J. Biomed. Mater. Res., Part B* **2012**, *100B*, 1451−1457.

(11) Paradossi, G.; Cavalieri, F.; Chiessi, E.; Spagnoli, C.; Cowman, M. K. Poly (vinyl alcohol) as versatile biomaterial for potential biomedical applications. *J. Mater. Sci.: Mater. Med.* **2003**, *14*, 687−691.

(12) Alexandre, N.; Ribeiro, J.; Gärtner, A.; Pereira, T.; Amorim, I.; Fragoso, J.; Lopes, A.; Fernandes, J.; Costa, E.; Santos-Silva, A.; Rodrigues, M.; Santos, J. D.; Maurício, A. C.; Luís, A. L. Biocompatibility and hemocompatibility of polyvinyl alcohol hydrogel used for vascular grafting–In vitro and in vivo studies. *J. Biomed. Mater. Res., Part A* **2014**, *102*, 4262−4275.

(13) Rynkowska, E.; Fatyeyeva, K.; Marais, S.; Kujawa, J.; Kujawski, W. Chemically and thermally crosslinked PVA-based membranes: effect on swelling and transport behavior. *Polymers* **2019**, *11*, 1799.

(14) Ashraf, A. A.; Zebarjad, S. M.; Hadianfard, M. J. The cross-linked polyvinyl alcohol/hydroxyapatite nanocomposite foam. *J. Mater. Res. Technol.* **2019**, *8*, 3149−3157.

(15) Hassan, C. M.; Peppas, N. A. Structure and Applications of Poly (vinyl alcohol) Hydrogels Produced by Conventional Cross-linking or by Freezing/Thawing Methods. In *Biopolymers PVA Hydrogels, Anionic Polymerisation Nanocomposites*; Springer: Berlin, Heidelberg, 2000; Chapter 3, Vol. *153*, DOI: 10.1007/3-540-46414-X_2.

(16) Kumeta, K.; Nagashima, I.; Matsui, S.; Mizoguchi, K. Crosslinking of Poly (vinyl alcohol) via Bis (β-hydroxyethyl) Sulfone. *Polymer J.* **2004**, *36*, 472−477.

(17) Kaur, J.; Saxena, M.; Rishi, N. An Overview of Recent Advances in Biomedical Applications of Click Chemistry. *BioconjugateChem.* **2021**, *32*, 1455−1471.

(18) Nwe, K.; Brechbiel, M. W. Growing applications of "click chemistry" for bioconjugation in contemporary biomedical research. *Cancer Biother. Radiopharm.* **2009**, *24*, 289−302.

(19) Moses, J. E.; Moorhouse, A. D. The growing applications of click chemistry. *Chem. Soc. Rev.* **2007**, *36*, 1249−1262.
(20) Hoyle, C. E.; Bowman, C. N. Thiol−ene click chemistry. *Angew. Chem., Int. Ed.*. **2010**, *49*, 1540−1573.
(21) Dicharry, R. M.; Ye, P.; Saha, G.; Waxman, E.; Asandei, A. D.; Parnas, R. S. Wheat Gluten- Thiolated poly (vinyl alcohol) blends with improved mechanical properties. *Biomacromolecules* **2006**, *7*, 2837−2844.
(22) Reesha, K. Sree Chitra Tirunal Institute for Medical Sciences and Technology. *Doctoral Thesis*, 2016.
(23) Pineda-Castillo, S.; Bernal-Ballén, A.; Bernal-López, C.; Segura-Puello, H.; Nieto-Mosquera, D.; Villamil-Ballesteros, A.; Muñoz-Forero, D.; Munster, L. Synthesis and characterization of poly (vinyl alcohol)-chitosan-hydroxyapatite scaffolds: a promising alternative for bone tissue regeneration. *Molecules* **2018**, *23*, 2414.
(24) Wei, Q.; Wang, Y.; Li, X.; Yang, M.; Chai, W.; Wang, K.; Zhang, Y. Study the bonding mechanism of binders on hydroxyapatite surface and mechanical properties for 3DP fabrication bone scaffolds. *J. Mech. Behav. Biomed. Mater.* **2016**, *57*, 190−200.
(25) Raz, P.; Brosh, T.; Ronen, G.; Tal, H. Tensile properties of three selected collagen membranes. *BioMed Res. Int.* **2019**, *2019*, No. 5163603.
(26) Kokubo, T.; Takadama, H. How useful is SBF in predicting in vivo bone bioactivity? *Biomaterials* **2006**, *27*, 2907−2915.
(27) Heydary, H. A.; Karamian, E.; Poorazizi, E.; Heydaripour, J.; Khandan, A. Electrospun of polymer/bioceramic nanocomposite as a new soft tissue for biomedical applications. *J. Asian Ceram. Soc.* **2015**, *3*, 417−425.
(28) RajeswariKrishnankutty, A.; NajeemaSulaiman, S.; Sadasivan, A.; Joseph, R.; Komath, M. Porous membranes of quaternized chitosan composited with strontium-based nanobioceramic for periodontal tissue regeneration. *J. Biomater. Appl.* **2022**, *36*, 1254−1268.
(29) Iviglia, G.; Cassinelli, C.; Torre, E.; Baino, F.; Morra, M.; Vitale-Brovarone, C. Novel bioceramic-reinforced hydrogel for alveolar bone regeneration. *Acta Biomater.* **2016**, *44*, 97−109.

https://doi.org/10.1021/acsomega.2c03382
ACS Omega 2022, 7, 29246−29255